

HES1 regulates bone marrow mesenchymal stromal cell function by suppressing NFATc2-mediated inflammation

Anthony Z. Zhu,^{1,2*} Zhilin Ma,^{3*} Emily V. Wolff,^{1,2,4*} Sanghoon Lee,^{1,2} Zichen Lin,⁵ Zhenxia J. Gao^{1,2} and Wei Du^{1,2}

¹Division of Oncology, University of Pittsburgh School of Medicine, Pittsburgh, PA; ²UPMC Hillman Cancer Center, Pittsburgh, PA; ³Department of Biological Sciences, University of Notre Dame, Notre Dame, IN; ⁴Graduate Program, Pennsylvania State University School of Medicine, Hershey, PA and ⁵Master of Science in Medical Science, Boston University School of Medicine Graduate Master Program, Boston, MA, USA

**AZZ, ZM and EVW contributed equally as first authors.*

Correspondence: Wei Du
wed41@pitt.edu

Received: May 15, 2025.

Accepted: September 24, 2025.

Early view: December 4, 2025.

<https://doi.org/10.3324/haematol.2025.288138>

©2026 Ferrata Storti Foundation

Published under a CC BY-NC license



Supplementary material

Flow cytometry

Bone marrow (BM) mesenchymal stroma cell (MSC) populations were stained with fluorescently labelled antibodies for mesenchymal (CD29, CD44, CD73, SCA-1, CD106) and hematopoietic markers (CD45, CD11b) using the mouse multipotent mesenchymal stromal cell marker antibody panel (Cat # SC018; R&D systems; Minneapolis, MN; 1-3). We confirmed that at least 98% MSC purity was obtained with this culture method.

For donor derived chimera analysis, peripheral blood (PB) from the recipient mice were subjected to staining using PE-anti-CD45.1, APC-anti-CD45.2 (Both from BD Biosciences, Cat #: 553776 and 558702, San Jose, CA) antibodies followed by Flow cytometry analysis.

For apoptosis staining, surface marker-stained cells were incubated with Annexin V and 7AAD using the BD ApoAlert Annexin V Kit (BD Pharmingen, San Jose, CA) in accordance with the manufacturer's instruction. Flow cytometry analysis was then performed to determine the proportion of Annexin V-positive cells.

For cell cycle analysis, cells stained for surface markers were fixed and permeabilized with Cytofix/Cytoperm buffer (BD Pharmingen) followed by intensive wash using Perm/Wash Buffer (BD Pharmingen). Anti-mouse Ki67 antibody (BD Pharmingen) and DAPI (Sigma-Aldrich) were then used to incubate the cells followed by flow cytometry analysis.

MSC Culture and Lineage Differentiation Assays

To measure the frequency of MSCs in the BM, colony forming unit fibroblast (CFU-F) assay was performed as previously described (4). Briefly, 4×10^6 bone marrow

mononuclear cells (BMMNCs) were plated into 6-well tissue culture plates in triplicate for each condition in mouse MesenCult medium (MesenCult basal media plus 20% of MesenCult Supplemental, Stem Cell Technologies Inc.) and incubated at 37°C and 5% CO₂. After 10 days of culture, medium was removed and each well was washed with phosphate-buffered saline (PBS), stained with 0.5% crystal violet solution (Fisher Scientific Company, VA, USA) according to the manufacturer's instructions and photographed.

For CFU-osteoblast assays, after 7 days of culture, medium was removed and switched to osteogenic differentiation medium (MesenCult medium supplemented with 10⁻⁷ M dexamethasone, 50 µg/mL ascorbic acid and 10 mM β-glycerophosphate). Medium was changed every other day for one week of continuous culture. Staining for ALP activity was subsequently performed using a Leukocyte Alkaline Phosphatase (ALP) kit according to the manufacturer's instructions (2, 3). Photomicrographs of the stained cells were acquired with a Nikon TE2000-S microscope. The area and intensity of ALP+ cells were quantified using Image J software.

For CFU-adipocyte assays, after 5 days of culture, medium was changed to adipogenic differentiation medium (MesenCult medium supplemented with 10⁻⁷ M dexamethasone, 450 µM isobutylmethylxanthine, 1 µg/mL insulin and 200 µM indomethacin). Culture medium changes every 5 days for 4 weeks. Adipocytes were determined by Oil Red O staining (5, 6).

RNA-seq data generation and pre-process

Qiagen RNeasy kit was used to extract total RNA from mouse MSCs. We calculated total RNA concentration and assessed the integrity. A library was independently prepared with

1 μ g of total RNA for each sample by Illumina TruSeq Stranded mRNA Sample Prep Kit (Illumina, Inc., San Diego, CA, USA, #RS-122-2101). The libraries were quantified using KAPA Library Quantification kits for Illumina Sequencing platforms according to the qPCR Quantification Protocol Guide (KAPA BIOSYSTEMS, KK4854) and qualified using the TapeStation D1000 ScreenTape (Agilent Technologies, 5067-5582). Indexed libraries were then submitted to an Illumina NextSeq Mid-Output sequencing kit (Illumina, Inc., San Diego, CA, USA), and the paired-end (2 \times 50 bp) sequencing was performed by the University of Pittsburgh sequencing core.

The raw RNA-seq data are available through the Gene Expression Omnibus (GEO) database under the accession number GSE296738. For analysis we used Rsubread (Bioconductor release 3.8; 7) to align sequence reads to reference genome and used edgeR (8) and limma (9) R packages (Bioconductor release 3.8) to normalize gene expression level to log₂ transcripts per million (TPM) (10). We aligned sequence reads to Mus Musculus genome reference sequence (GCF_000001635.27_GRCm39) downloaded from NCBI assembly database and mapped the aligned sequences to gene symbols. After normalization, we contained only protein-coding genes and removed genes of which expression level is zero across all samples to get 26,938 genes for further pathway analysis.

Functional assessment for DEGs and gene set enrichment analysis

To explore the gene expression profile of the effect of *Hes1* KO in the BM MSC, statistical significance of the differential expression data was determined using DESeq2 and fold change. False discovery rate (FDR) was controlled by adjusting *p* value using Benjamini-Hochberg algorithm. The log₂ fold change and *p*-value obtained from the comparison of

each group plotted as the volcano plot. Hierarchical clustering analysis was performed using complete linkage and Euclidean distance as a measure of similarity. The significant different expression genes (DEGs) were aggregated using the DESeq2 on read counts and the genes were represented in the hierarchical clustering heatmap using the “complete” distance metric for the clustering algorithm. We used ComplexHeatmap R package for the visualization (11). All data analysis and visualization of differentially expressed genes was conducted using R version 4.3.3 (12).

For deep functional assessment of the enriched gene signatures, the DEGs identified between wild type and *Hes1* KO were applied to Gene Signature Enrichment Analysis (GSEA) with Hallmark gene signatures (version 6.2 at MSigDB, <http://software.broadinstitute.org/gsea>) (13). The pathway network was visualized using the igraph (ver. 2.0.3; 14) and IndepthPathway (ver. 1.0; 15).

Master regulator analysis (MRA) using mouse bone marrow mesenchymal stem cell (MSC)-specific transcriptional interactome

Algorithm for the Reconstruction of Gene Regulatory Networks (ARACNe) algorithm was used to construct MSC-specific transcriptional interactome as described in our previous papers (16, 17). The *Rattus norvegicus* transcription factors (TFs) were collected from Animal Transcription Factor Database 3.0 (AnimalTFDB 3.0). From the combined microarray data of GSE87439, GSE15713, and GSE21573, a consensus gene network was generated by 100 rounds of ARACNe bootstrapping (<http://califano.c2b2.columbia.edu/aracne/>). MRA-Fisher’s exact test (FET) was used to infer master regulator candidates and their transcriptional targets in A7r5 cell-specific transcriptional interactome. The ARACNe preprocessing and MRA-FET analysis were

run in geWorkbench software version 2.6.0 (<http://wiki.c2b2.columbia.edu/workbench/index.php/Home>)

Assessment of ligand - receptor interactions (CellPhoneDB).

We used CellPhoneDB (version 3.1.0; 18) to identify the potential ligand–receptor interactions for bone marrow MSC KO environment based on the raw count matrices. For WT and Hes1 KO groups, the means expression of interacting ligands in the sender population and interacting receptors in the receiver population were computed, and a one-sided Wilcoxon signed-rank test was used to assess the statistical significance of each interaction score.

ELISA

Whole bone marrow cells (WBMCs) from one femur were collected from the indicated mice 24h post 500 cGy TBI. After centrifugation, BM supernatants were collected into Iove's modified Dulbecco's medium (IMDM) and analyzed for TNF- α , CXCL4, IL-1 β or CCL11 concentration using ELISA kit (Cat# MTA00B; MAB350; MLB00C and MME00; R&D systems) following the manufacturer's instruction.

Reporter gene assays

A total of 10^6 MSCs from *Hes1*-KO mice were transfected with a NFATc2 reporter construct containing 1.5 kB of the proximal NFATc2 promoter, pGL3-KB-Luc (NFAT Luciferase reporter (Addgene; 19) and plated on a 6-well plate. After 48 hours, cells were incubated with the indicated proteins (30 μ g/mL). The cells were harvested 12 hours after treatment, washed with PBS, and luciferase activity was assessed using the dual luciferase assay reporter kit (Promega, Madison, WI).

Chromatin immunoprecipitation (ChIP)

ChIP assays were performed using a Magna ChIP A/G Chromatin Immunoprecipitation Kit (Millipore, Billerica, MA, USA; No. 17-10085) according to the protocol (20). Briefly, the cells were treated with 1% formaldehyde for 10 min at room temperature to cross-link DNA and proteins, and 125 mM glycine was used to quench residual formaldehyde for 5 min. After the wells were washed with cold PBS, they were lysed in lysis buffer for 15 min on ice. Then, crosslinked DNA in the lysates was sheared to fragments of 200 ~ 1000 base pairs (bp) by sonication (six times, 15 s each time with 50 s rest). The obtained samples were immunoprecipitated with anti-HES1 antibody (Novus Biologicals, Centennial, CO; NBP1-47791) or anti-IgG antibody (Cell Signalling Technology, Boston, MA, USA; No. 2729s) overnight at 4°C. Immunoprecipitated complexes were collected using Protein A/G magnetic beads. The complex was digested by proteinase K at 65°C for 2 h, and beads were separated by a magnetic device. Then, DNA fragments were purified and assessed by PCR and agarose gel electrophoresis. The sequences of primers used for PCR were synthesized by IDT and are listed in Supplementary Table S2. RNA extraction and quantitative real-time polymerase chain reaction (qRT-PCR; 21).

Statistical analysis

Paired or unpaired student's *t-test* was used for two-group comparisons. Survival data were plotted by the Kaplan-Meier curve method and analyzed by the log-rank test. Values of $p < 0.05$ were considered statistically significant. Results are presented as mean \pm SD. * indicates $p < 0.05$; ** indicates $p < 0.01$.

References:

1. Huang S, Xu L, Sun Y, et al. An improved protocol for isolation and culture of mesenchymal stem cells from mouse bone marrow. *J Orthop Transl.* 2015;3:26-33.
2. Delorme B, Ringe J, Gallay N, et al. Specific plasma membrane protein phenotype of culture-amplified and native human bone marrow mesenchymal stem cells. *Blood.* 2008;111:2631-2635.
3. Houlihan DD, Mabuchi Y, Morikawa S, et al. Isolation of mouse mesenchymal stem cells on the basis of expression of Sca-1 and PDGFR- α . *Nat Protoc.* 2012;7:2103-2111.
4. Wu X, Estwick SA, Chen S, et al. Neurofibromin plays a critical role in modulating osteoblast differentiation of mesenchymal stem/progenitor cells. *Hum Mol Genet.* 2006;15:2837-2845.
5. Zhang P, Xing C, Rhodes SD, et al. Loss of *Asxl1* Alters Self-Renewal and Cell Fate of Bone Marrow Stromal Cells Leading to Bohring-Opitz-like Syndrome in Mice. *Stem Cell Rep.* 2016;6(6):914-925.
6. Zhang P, Chen Z, Li R, et al. Loss of *ASXL1* in the bone marrow niche dysregulates hematopoietic stem and progenitor cell fates. *Cell Discov.* 2018;4:4.
7. Liao Y, Smyth GK, Shi W. The Subread aligner: fast, accurate and scalable read mapping by seed-and-vote. *Nucleic Acids Res.* 2013;41(10):e108-e108.
8. McCarthy DJ, Chen Y, Smyth GK. Differential expression analysis of multifactor RNA-Seq experiments with respect to biological variation. *Nucleic Acids Res.* 2012;40(10):4288-4297.
9. Ritchie ME, Phipson B, Wu D, et al. limma powers differential expression analyses for RNA-sequencing and microarray studies. *Nucleic Acids Res.* 2015;43(7):e47-e47.
10. Wagner GP, Kin K, Lynch VJ. Measurement of mRNA abundance using RNA-seq data: RPKM measure is inconsistent among samples. *Theory Biosci.* 2012;131(4):281-285.
11. Gu Z, Eils R, Schlesner M. Complex heatmaps reveal patterns and correlations in multidimensional genomic data. *Bioinformatics.* 2016;32(18):2847-2849.
12. Team RC. R: A Language and Environment for Statistical Computing. R Foundation for Statistical Computing, Vienna 2021. <https://www.R-project.org>.
13. Subramanian A, Tamayo P, Mootha VK, et al. Gene set enrichment analysis: a knowledge-based approach for interpreting genome-wide expression profiles. *Proc Natl Acad Sci U S A.* 2005;102(43):15545-15550.
14. Csardi MG: Package 'igraph'. Last accessed 2013;3(09):2013.
15. Lee S, Deng L, Wang Y, Wang K, Sartor MA, Wang X-S. InDepthPathway: an integrated tool for in-depth pathway enrichment analysis based on single-cell sequencing data. *Bioinformatics.* 2023;39(6):btad325.
16. Lee S, Chun JN, Kim SH, So I, Jeon JH. Icilin inhibits E2F1-mediated cell cycle regulatory programs in prostate cancer. *Biochem Biophys Res Commun.* 2013;441(4):1005-10
17. Lee S, Park YR, Kim SH, et al. Geraniol suppresses prostate cancer growth through down-regulation of E2F8. *Cancer Med.* 2016 Oct;5(10):2899-2908.

18. Efremova M, Vento-Tormo M, Teichmann SA, Vento-Tormo R: CellPhoneDB: inferring cell-cell communication from combined expression of multi-subunit ligand-receptor complexes. *Nat Protocols*. 2020;15(4):1484-1506.
19. Ichida M, Finkel T. Ras regulates NFAT3 activity in cardiac myocytes. *J Biol Chem*. 2001. 276(5):3524-3530.
20. Wu L, Li X, Lin Q, Chowdhury F, Mazumder MH, Du W. FANCD2 and HES1 suppress inflammation-induced PPAR γ to prevent haematopoietic stem cell exhaustion. *Br J Hematol*. 2021;192(3):652-663
21. Sharma D, Mirando AJ, Leinroth A, Long JT, Karner CM, Hilton MJ. HES1 is a novel downstream modifier of the SHH-GLI3 axis in the development of preaxial polydactyly. *PloS Genet*. 2021;17(12):e1009982.

Supplementary tables

Table S1. Steady state hematological parameter of *Hes1^{fl/fl}Prx1Cre* mice.

	Absolute and differential WBC counts				Characterization of red blood cells				Plts
	WBC(cells/ul)	Lymphocyte (%)	Neutrophils (%)	Monocytes (%)	RBC (X10 ¹² /L)	HCT (%)	MCV (fL)	Hb (g/dL)	(X10 ⁹ /L)
<i>Hes1^{fl/fl}</i>	7.15±2.24	61.2±8.5	27.1±14	3.82±2.1	8.16±1.13	43.8±6.71	53.91±1.72	12.49±1.5	608.1±187
<i>Hes1-KO</i>	8.732±3.41	61.08±21	34.17±21	4.945±1	8.71±1.72	44.93±8.05	52.08±3.18	12.93±2.7	761.2±240
<i>P</i>	0.5673	0.2615	0.5263	0.3531	0.413	0.718	0.4044	0.615	0.26961

Table S2. qPCR primers

	Primers used for qPCR	
Gene	Forward	Reverse
<i>Hes1</i>	GGAAATGACTGTGAAGCACCTCC	GAAGCGGGTCACCTCGTTCATG
<i>Nfatc2</i>	ACTTCACAGCGGAGTCCAAGGT	GGATGTGCTTGTTCCGATACTCG
<i>Tnfa</i>	GGTGCCTATGTCTCAGCCTCTT	GCCATAGAAGTATGAGAGGGAG
<i>Cxcl4</i>	GTTGTTTCTGCCAGCGGTGGTT	ACAGTGGCGTCCTGCCTTGATC
<i>Il1b</i>	TGGACCTTCCAGGATGAGGACA	GTTTCATCTCGGAGCCTGTAGTG
<i>Ccl11</i>	TCCATCCCAACTTCCTGCTGCT	CTCTTTGCCAACCTGGTCTTG
<i>Gapdh</i>	TCAATGAAGGGGTCGTTGAT	CGTCCCGTAGACAAAATGGT
	Primers used for ChIP assay	
Gene	Forward	Reverse
<i>N Class E box</i>	TGGGAAGTTTCACACGAGCC	ATCTGCCATTTACCCCGAG
<i>B class E box</i>	TCCGTCAGCCGGAAGTACAG	CAACTTCTGCTTCACCTGCT

Supplementary figures

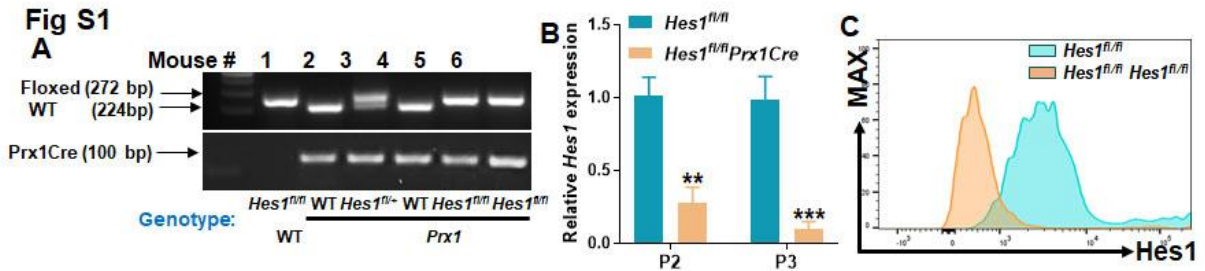


Fig S1. Validation of MSC specific *Hes1* deletion. A. Genotyping of *Hes1^{fl/fl}Prx1Cre* mice and their *Hes1^{fl/fl}* littermates. Genomic DNA was extracted from tails collected from *Hes1^{fl/fl}Prx1Cre* mice and their *Hes1^{fl/fl}* littermates followed by PCR reaction. DNA gel image indicates expected PCR products for WT allele (224bp) and floxed allele (272 bp). B. qPCR verifies *Hes1* deletion in MSCs. RNA was extracted from MSCs (Passage 2, Left; Passage 3, Right) isolated from *Hes1^{fl/fl}Prx1Cre* mice and their *Hes1^{fl/fl}* littermates followed by qPCR analysis for *Hes1*. Samples were normalized to the level of *GAPDH* mRNA. C. Intercellular *Hes1* staining. MSCs from *Hes1^{fl/fl}Prx1Cre* mice and their *Hes1^{fl/fl}* littermates were subjected to intracellular *Hes1* staining after passaged twice in *ex vivo* culture.

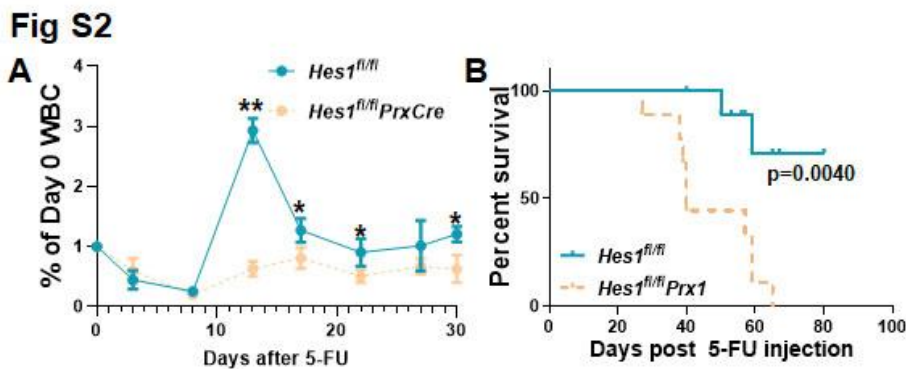


Fig S2. *Hes1^{fl/fl}Prx1Cre* mice are hypersensitive to 5-FU challenge. A. *Hes1^{fl/fl}Prx1Cre* mice exhibit lagging recovery kinetics after 5-FU injection. The white blood cell (WBC)

count of *Hes1^{fl/fl}* and *Hes1^{fl/fl}Prx1Cre* mice after a single injection of 5-FU (150 mg/kg) was monitored over time. B. *Hes1^{fl/fl}Prx1Cre* mice are hypersensitive to 5-FU treatment. 5-FU (135 mg/kg) was administrated to *Hes1^{fl/fl}Prx1Cre* mice and their *Hes1^{fl/fl}* and *Hes1^{fl/fl}* littermates weekly for 3 consecutive weeks. Survival of the animals was plotted by the Kaplan-Meier curve method and analyzed by the log-rank test.

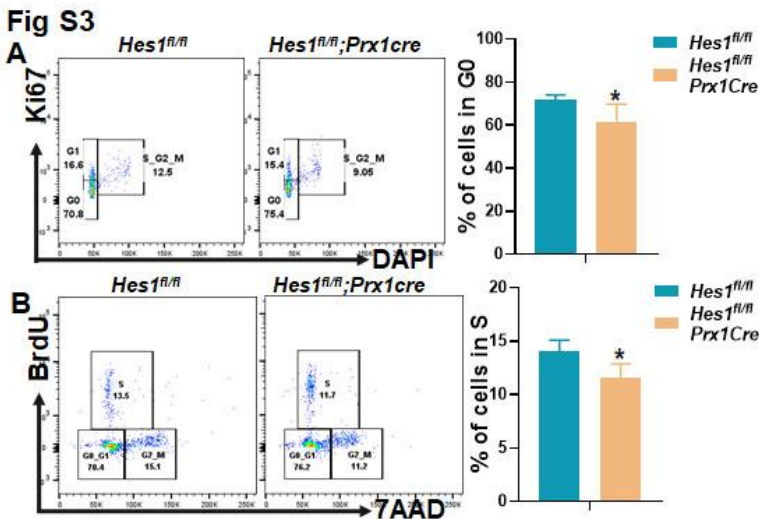


Fig S3. MSCs from *Hes1^{fl/fl}Prx1Cre* mice are more quiescent. WBMCs from *Hes1^{fl/fl}Prx1Cre* and *Hes1^{fl/fl}* mice were subjected to flow cytometry analysis for ki67 and DAPI (A) and BrdU incorporation (B). Representative flow plot (Left) and quantification (Right) are shown.

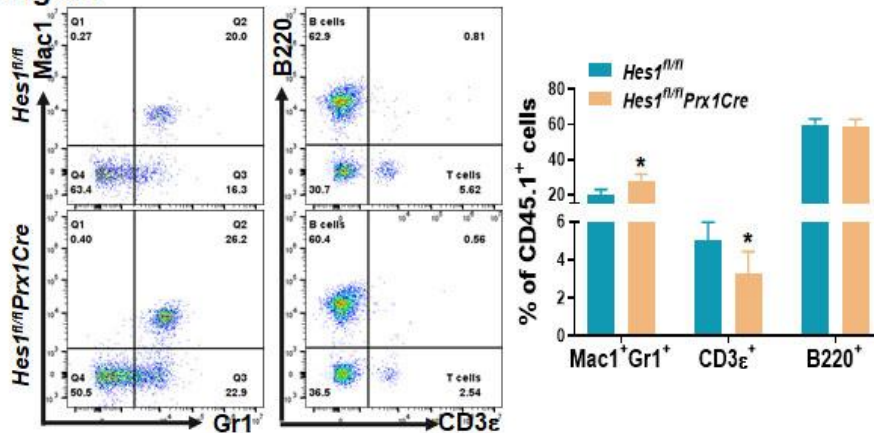
Fig S4

Fig S4. Lineage differentiation in BMT recipients. WBMCs from BoyJ mice (CD45.1⁺) were transplanted into lethally irradiated *Hes1^{fl/fl}Prx1Cre* and *Hes1^{fl/fl}* mice. Lineage differentiation in *Hes1^{fl/fl}Prx1Cre* recipients. PB from the recipient mice described in B were subjected to flow cytometry for CD3ε/B220, Gr1/Mac1.

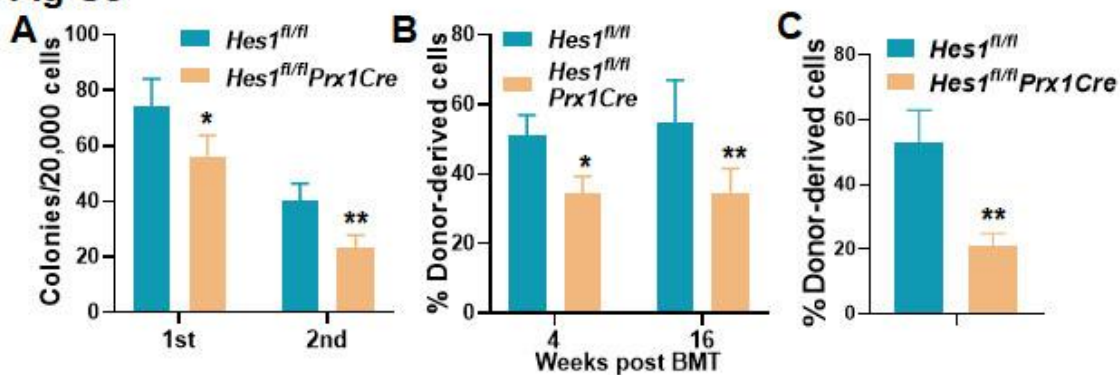
Fig S5

Fig S5. HSPCs from *Hes1^{fl/fl}Prx1Cre* mice are functionally defective. A. Loss of *Hes1* in BM niche affects HSPC progenitor activity. WBMCs from *Hes1^{fl/fl}Prx1Cre* or *Hes1^{fl/fl}* mice were plated in cytokine-supplemented methylcellulose medium. Colonies were enumerated on day 7. Results are means ± standard deviation (SD) of three independent experiments (n = 6~9 per group). B. Mesenchymal *Hes1* deletion compromises

hematopoietic reconstitution in the recipients. WBMCs, along with 2×10^5 competitor cells from congenic BoyJ mice were transplanted into lethally irradiated BoyJ recipients. Donor-derived chimera was detected 16 weeks post BMT. *C. Hes1* deletion impair long-term reconstitution. WBMCs from the primary recipients described in B were transplanted into sublethally irradiated BoyJ recipients. 2nd BMT. Donor-derived chimera was detected 16 weeks post BMT.

Supplementary Figure 6

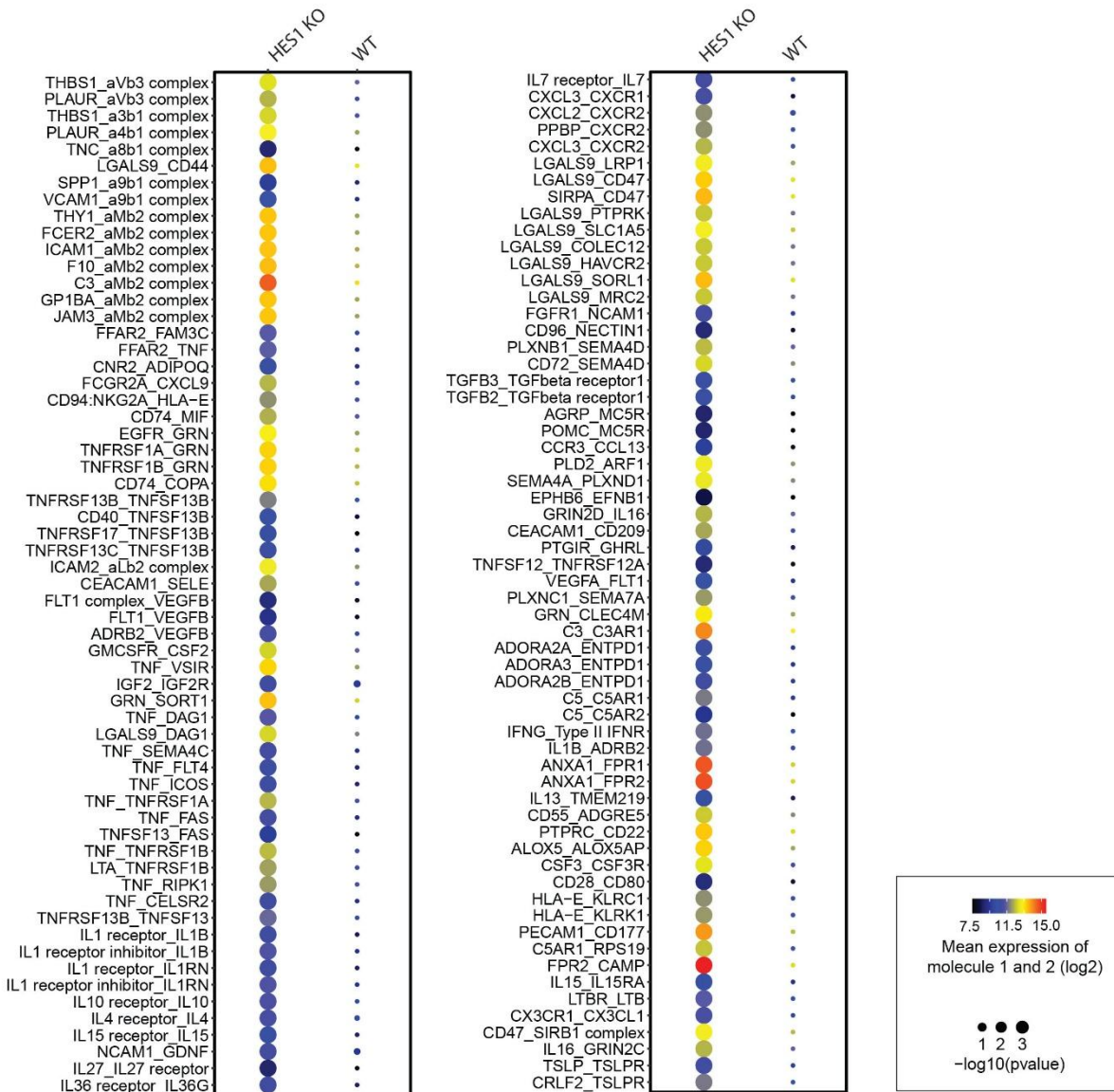


Fig S6. Inflammation panel. CellPhoneDB analysis was conducted to identify gene pairs of ligand-receptor expressed in the BM cells using the RNA-seq data described in Fig 5. Using CellPhoneDB pipeline, statistically significant mean expression of ligand-receptor genes was determined in *Hes1*-KO or control group. Size indicates $-\log_{10}(p\text{-values})$, and color indicates the mean expression of the ligand-receptor pairs in individual groups.

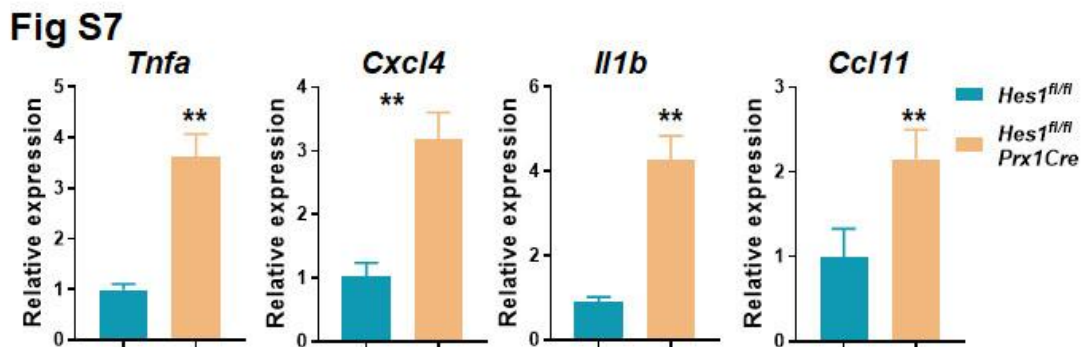


Fig S7. qPCR analysis of inflammatory genes identified from transcriptomics analysis. RNA extracted from MSCs, isolated from *Hes1^{fl/fl}Prx1Cre* mice and their *Hes1^{fl/fl}* littermates were subjected to quantitative RT-PCR using primers listed in Table S2. Samples were normalized to the level of *GAPDH* mRNA.

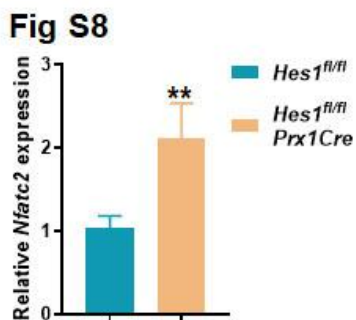


Fig S8. Reduced NFATc2 in *Hes1*-KO MSCs. RNA was extracted from MSCs (Passage 2) isolated from *Hes1^{fl/fl}Prx1Cre* mice and their *Hes1^{fl/fl}* littermates followed by qPCR analysis for *Nfatc2*. Samples were normalized to the level of *GAPDH* mRNA.